Available online at www.sciencedirect.com
ScienceDirect
ELSEVIER
Journal of the European Ceramic Society 28 (2008) 2099–2107
ECERS
www.elsevier.com/locate/jeurceramsoc

Surface strengthening of Ti_3SiC_2 through magnetron sputtering Cu and subsequent annealing

Haiping Guo [a,b], Jie Zhang [a,c], Fangzhi Li [a,c], Yi Liu [b], Jinjie Yin [b], Yanchun Zhou [a,*]

[a] Shenyang National Laboratory for Materials Science, Institute of Metal Research, Chinese Academy of Sciences, 72 Wenhua Road, Shenyang 110016, China
[b] Liaoning Technical University, Fuxin 123000, China
[c] Graduate School of Chinese Academy of Science, Beijing 100039, China

Received 9 September 2007; received in revised form 10 January 2008; accepted 1 February 2008
Available online 18 April 2008

Abstract

Magnetron sputtering deposition Cu and subsequent annealing in the temperature range of 900–1100 °C for 30–60 min were conducted with the motivation to modify the surface hardness of Ti_3SiC_2. Owing to the formation of TiC following the reaction $Ti_3SiC_2 + 3Cu \rightarrow 3TiC_{0.67} + Cu_3Si$, the surface hardness was enhanced from 5.08 GPa to a maximum 9.65 GPa. In addition, the surface hardness was dependent on the relative amount of TiC, which was related to Cu film thickness, heat treatment temperatures and durations of annealing. Furthermore, after annealing at 1000 °C for 30 min the Cu-coated Ti_3SiC_2 has lower wear rate and lower COF at the running-in stage compared with Ti_3SiC_2 substrate. The reaction was triggered by the inward diffusion of Cu along the grain boundaries and defects of Ti_3SiC_2. At low temperature and short annealing time, i.e. 900 or 1000 °C for 30 min, Cu diffused inward Ti_3SiC_2 and accumulated at the trigonal junctions first. At higher temperature of 1100 °C or prolonging the annealing time to 60 min, considerable amount of Cu diffused to Ti_3SiC_2 and filled up the grain boundaries leaving a mesh structure.
© 2008 Elsevier Ltd. All rights reserved.

Keywords: Ti_3SiC_2; Surface strengthening; Magnetron sputtering; Microhardness; Tribological property

1. Introduction

In recent years, layered ternary carbides and nitrides, such as Ti_3SiC_2, Ti_3AlC_2, Ti_2AlC, Ti_2SnC and Ti_2AlN, are attracting much attention owing to their unique combination of properties of both metals and ceramics. They have been recognized as materials for potential applications in various industrial fields. Among all these compounds, Ti_3SiC_2 has been most extensively investigated. It has low density, good thermal and electrical conductivity, high elastic moduli and easy machinability.[1–4] However, compared with traditional binary carbides, for instance TiC, its hardness and wear resistance are relatively low, which limit its widespread applications. Therefore, surface strengthening to modify the properties of Ti_3SiC_2 without losing its intrinsic merits is of vital importance.

In order to enhance the surface hardness of Ti_3SiC_2, El-Raghy and Barsoum[5] altered its surface chemistry through two ways: carburization and silicidation. Reaction of Ti_3SiC_2 with graphite foils in the temperature range of 1400–1600 °C resulted in the formation of a 15 vol.% porous surface layer of TiC_x (where $x > 0.8$), which increased the surface hardness from 4 to 20–25 GPa. While in the process of silicidation, reaction of Ti_3SiC_2 with silicon wafers in the temperature range of 1200–1350 °C resulted in the formation of a dense surface layer composed of a two-phase mixture of $TiSi_2$ and SiC, which also increased the surface hardness to 10–12 GPa. Li et al.[6] improved the surface hardness and wear resistance of Ti_3SiC_2 by boronizing treatment, which was carried out through powder pack cementation in the temperature range of 1100–1400 °C. A maximal hardness of 9.3 GPa was obtained with the formation of a layer of TiB_2 and β-SiC mixture, meanwhile its wear resistance was also significantly improved.

It is well known that the crystal structure of Ti_3SiC_2 can be considered as two-dimensional closed packed layers of Si periodically intercalated into the (1 1 1) twin boundary of $TiC_{0.67}$ (Ti_3C_2).[7] The de-intercalation of Si from Ti_3SiC_2 caused the

* Corresponding author. High-performance Ceramic Division, Shenyang National Laboratory for Materials Science, Institute of Metal Research, Chinese Academy of Sciences, 72 Wenhua Road, Shenyang 110016, China.
Tel.: +86 24 23971765; fax: +86 24 23891320.
E-mail address: yczhou@imr.ac.cn (Y. Zhou).

0955-2219/$ – see front matter © 2008 Elsevier Ltd. All rights reserved.
doi:10.1016/j.jeurceramsoc.2008.02.011

topological transformation from hexagonal Ti_3SiC_2 to cubic $TiC_{0.67}$. Obviously, when the de-intercalation takes place, the as-formed TiC will increase the hardness of Ti_3SiC_2. Thus the motivation for this work is to induce the topological transformation at the surface of Ti_3SiC_2, which could take place when it contacts in Cu,[8] Ni,[9] graphite,[5] molten cryolite[10] and liquid Al.[11] Since Cu films can be deposited readily by magnetron sputtering, which is a well-established technology with lower working gas pressure and higher sputtering rate,[12] in the present work, to enhance the surface hardness and wear resistance, a thin layer of Cu was deposited on Ti_3SiC_2 followed by annealing at high temperature. In addition, the reaction products, microstructure, Vickers hardness and tribological properties of the reaction layer were investigated.

2. Experimental procedures

2.1. Substrate material

The bulk Ti_3SiC_2 used in this work was fabricated by an in situ hot pressing/solid–liquid reaction process, which was described in detail elsewhere.[3] The measured density of Ti_3SiC_2 was 97% of the theoretical value, which was determined by the Archimedes' immersion method. The Ti_3SiC_2 substrate was cut into rectangular specimens of 8 mm × 8 mm × 2 mm by electrical discharge method from an as-fabricated bulk piece. The surfaces used for sputter deposition were ground down to 1500 grade SiC paper, mechanically polished using 1.5 μm diamond paste to ensure a flat and mirror-like surface, and then ultrasonically cleaned in ethanol and acetone individually for 10 min before they were transferred into the sputter chamber.

2.2. Deposition of Cu

A JGP560C14 ultrahigh vacuum (UHV) magnetron sputtering deposition system (SKY Technology Development Co. Ltd, Shenyang, China) was used in depositing polycrystalline Cu films onto Ti_3SiC_2 substrate. A schematic diagram of a direct current (dc) magnetron sputtering system used in the present work is shown in Fig. 1. Copper target of 99.99% purity with 60 mm in diameter was used. During deposition, the substrates were kept static with the substrate-to-target separation ($d_{s\text{–}t}$) of 60 mm to ensure an identical condition for each run. The sputtering chamber was evacuated to a base pressure of $\sim 5 \times 10^{-4}$ Pa, and then backfilled with high purity argon to the required coating pressure at 0.4–0.5 Pa with a gas flow rate of generally 20 sccm. Cu film deposition process was carried out under the dc power of 100 W, meanwhile a negative dc bias of 100 V was applied to the substrate. The detailed process parameters are listed in Table 1. Prior to deposition, the pure copper target was pre-sputtered for 5 min in order to remove the contaminants and oxides on the surface. During the target cleaning, a shield was interposed between the target and the substrate to avoid the substrate contamination. Although there was no deliberate attempt at heating the substrates, the temperature of the films rose as high as ∼70 °C during magnetron sputtering as a result of the condensing of the sputtered atoms—the heat of condensation plus their kinetic energy.

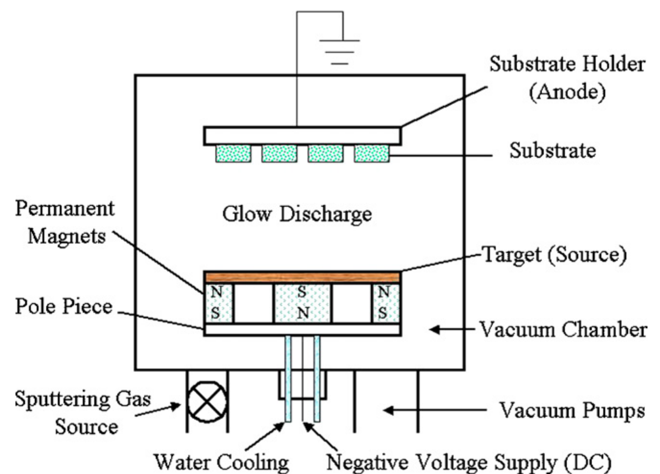

Fig. 1. Schematic illustration of a magnetron sputtering system.

2.3. Annealing process

After deposition, the Cu-coated Ti_3SiC_2 samples were annealed in order to obtain a layer composed of TiC and copper silicides. There was no apparent reaction between Ti_3SiC_2 and Cu at temperatures below 900 °C, according to previous work on high-temperature reaction between Ti_3SiC_2 and Cu by Zhou et al.[8] Thus, attention was only paid to the samples annealed at temperatures above 900 °C. In this work, Cu-coated Ti_3SiC_2 were annealed at various temperatures ranging from 900 to 1100 °C for 30–60 min in a horizontal tube furnace under flowing argon atmosphere. The detailed process parameters are listed in Table 2.

Table 1
Parameters for the deposition of Cu on Ti_3SiC_2 by magnetron sputtering method

Target source	Cu (diameter: 60 mm)
Substrate	Ti_3SiC_2 (dimension: 8 mm × 8 mm × 2 mm)
Sputtering gas	Ar
Base pressure (Pa)	5×10^{-4}
Gas partial pressure (Pa)	0.4–0.5
Gas flow rate (sccm)	20
dc sputtering power (W)	100
Negative dc bias applied to the substrate (V)	100
Substrate temperature[a] (°C)	70
Substrate-target distance (mm)	60
Deposition time (h)	2∼6
Deposition rate (μm/min)[b]	0.17

[a] Although there was no deliberate attempt at heating the substrates, the temperature of the films rose as high as ∼70 °C during magnetron sputtering as a result of the condensing of the sputtered atoms—the heat of condensation plus their kinetic energy.

[b] The thickness of the film is measured using a HXD-1000B digital microhardness tester and the growth rate is calculated from the film thickness obtained for a given deposition time.

Table 2
Annealing parameters of Cu-coated Ti_3SiC_2

Sputtering	Thickness of Cu Film (μm)	20	40	60
Annealing	Temperature (°C)	900	1000	1100
	Duration (min)	30	30	30
		60	60	60

2.4. Characterization of the reaction layer

X-ray diffraction (XRD, Rigaku D/max-2400, Japan) with Cu Kα radiation was used to identify the annealing-induced reaction products. Lattice parameters and relative amount of the phases in the reaction layer were calculated using the Rietveld method,[13] which was accomplished in a DBWS code in the Cerius[2] computational program for material research (Molecular Simulation Inc., USA). The intensity of the XRD profile is represented by

$$I_{\mathrm{Rietveld}}(2\theta) = b(2\theta) + s\sum_{K} L_K |F_K|^2 \phi(2\theta_i - 2\theta_K) P_K A_K \quad (1)$$

where $b(2\theta)$ is the background intensity, s is a scale factor, L_k contains the Lorentz, polarization and multiplicity factor, ϕ is the profile function, P_K is the preferred orientation function, A_K is the absorption factor and F_K is the structure factor. The subscript K represents Miller indices for the Bragg reflections.

A scanning electron microscope (SEM, LEO Super 35, Germany) equipped with an energy dispersive spectroscope (EDS) system was employed to investigate the morphological evolution of the surface and cross-section of the sample after annealing.

Vickers hardness of the reaction layer was determined by an HXD-1000B (Shanghai Taiming optical Inc., China) digital microhardness tester at a load of 1 N with a dwell time of 15 s. Ten measurements were carried out for each sample. The results were free from substrate effect according to the 1/10 rule.[14]

Tribological property was conducted on a ball-on-disk reciprocating type computerized fretting tribometer (CETR UMT-2, USA) at constant normal loads. The friction coefficient was obtained from the on-line measured tangential force. Ti_3SiC_2 and Ti_3SiC_2 with 40 μm Cu coating after annealing at 1000 °C for 30 min in the dimension of 16 mm × 4 mm × 3 mm were used as flat samples, which oscillated over the desired displacement. The commercial bearing AISI 52100 grade steel balls (hardness 55 HRC) of 4.76 in diameter were used as counterbody (stationary). Before each test, the specimen and ball were ultrasonically cleaned with acetone. The fretting wear experiments were carried out under varying loads (1 and 5 N) with constant testing duration (120 min), at constant frequency (3.3 Hz) and constant displacement stroke (8.46 mm). All tests were done in air at room temperature (28 ± 1 °C) with relative humidity of RH 49 ± 3%. After each test, the worn surfaces of both the flat and the ball were ultrasonically cleaned with acetone. The surface roughness was obtained by a stylus instrument (JB-4C precision surface roughness meter, Shanghai Taiming Optical Inc., China). From the estimated wear volume, the specific wear rates (wear volume/(load × total fretted distance)) were calculated.

3. Results

3.1. Reactions between Ti_3SiC_2 and Cu film

Fig. 2 shows the X-ray diffraction patterns of (a) Ti_3SiC_2 substrate, (b) Ti_3SiC_2 coated with 20 μm Cu, and (c–h) Cu-coated Ti_3SiC_2 after annealing in the temperature range of 900–1100 °C for 30 and 60 min. It is seen from Fig. 2a that a minor amount of TiC exists in the as-prepared Ti_3SiC_2 substrate. After sputtering for 2 h, only diffraction peaks of Cu for the as-deposited sample can be observed (Fig. 2b). Upon further annealing, in Fig. 2c–h, the Cu peaks disappear, while diffraction peaks of Cu_3Si simultaneously appear at 2θ values of 44.76° and 45.24° which can be assigned as Cu_3Si (3 2 0) and Cu_3Si (3 1 2).[15,16] Moreover, the peak intensity of TiC (2 0 0) also increases which indicates that TiC is one of the reaction products. Therefore, Ti_3SiC_2 reacted with Cu under the annealing conditions to form TiC and Cu–Si intermetallic compound Cu_3Si according to the following reaction:

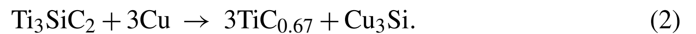

$$Ti_3SiC_2 + 3Cu \rightarrow 3TiC_{0.67} + Cu_3Si. \quad (2)$$

The relative amount and lattice parameters of Ti_3SiC_2 and TiC_x (here TiC_x is used owing to the wide homogeneous composition region of carbon) in Ti_3SiC_2 substrate and Cu-coated Ti_3SiC_2 after annealing were calculated using the Rietveld method. In all Rietveld simulations, it was performed using the cubic structure for TiC. Meanwhile, the reliability factors, i.e., R-P and R-WP values, are less than 10%, as shown in Table 3. After annealing at 1000 °C for 30 min, it can be seen that the

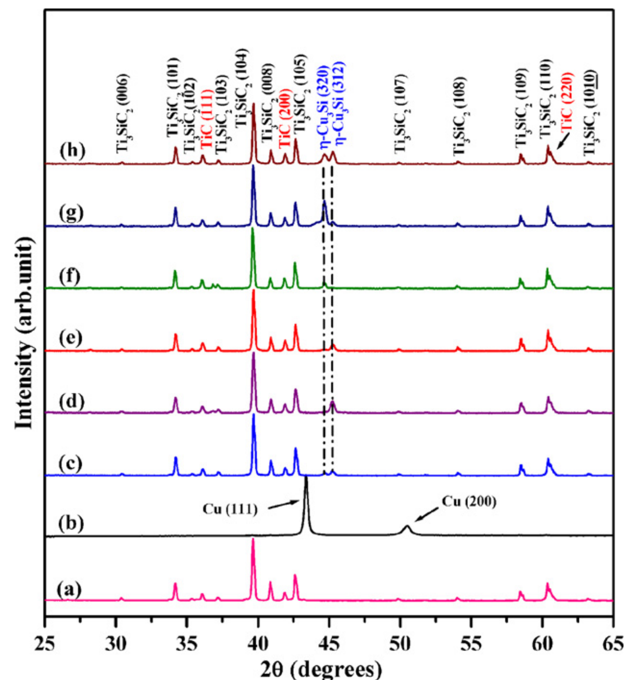

Fig. 2. X-ray diffraction patterns of (a) Ti_3SiC_2 substrate, (b) Ti_3SiC_2 coated with 20 μm Cu, (c) 20 μm Cu-coated Ti_3SiC_2 after annealing at 1000 °C for 30 min, 40 μm Cu-coated Ti_3SiC_2 after annealing at (d) 900 °C for 30 min, (e) 1000 °C for 30 min, (f) 1100 °C for 30 min, and (g) 1000 °C for 60 min, and (h) 60 μm Cu-coated Ti_3SiC_2 after annealing at 1000 °C for 30 min.

Table 3
Lattice parameters and relative content of Ti_3SiC_2 and TiC for Ti_3SiC_2 substrate and Cu-coated Ti_3SiC_2 after annealing

Sample	Ti_3SiC_2				TiC_x			Reliability factor	
	Lattice constants		$\Delta V/V$ (%)	Weight percent	Lattice constant a (Å)	x	Weight percent	R-P (%)	R-WP (%)
	a (Å)	c (Å)							
Ti_3SiC_2 substrate	3.06150	17.64850	0	80.1	4.31140	0.88	19.9	7.93	13.41
20 μm 1000 °C to 30 min	3.05860	17.63230	0.279	79.9	4.30770	0.69	20.1	6.29	8.56
40 μm 900 °C to 30 min	3.05980	17.63520	0.188	78.9	4.31030	0.81	21.1	6.02	9.78
40 μm 1000 °C to 30 min	3.05890	17.63500	0.244	76.1	4.30830	0.71	23.9	6.22	8.24
40 μm 1100 °C to 30 min	3.06150	17.64590	0.014	77.2	4.31070	0.82	22.8	5.31	7.03
40 μm 1000 °C to 60 min	3.06260	17.65110	−0.084	78.9	4.31280	1	21.1	6.27	8.95
60 μm 1000 °C to 30 min	3.05880	17.63220	0.265	72.7	4.30850	0.73	27.3	5.95	7.79

"20 μm 1000 °C to 30 min" in the first column denotes Ti_3SiC_2 coated with 20 μm Cu after annealing at 1000 °C for 30 min. So do the others.

relative amount of TiC_x increases with increasing the thickness of Cu films, i.e., 20.1, 23.9 and 27.3 wt.% for samples with a Cu film of 20, 40 and 60 μm, respectively. For a fixed Cu film thickness of 40 μm, the relative amount of TiC_x increases with increasing the heat treatment temperature below 1000 °C, and then drops appreciably at 1100 °C. Similar trend can be observed for the annealing duration changed from 30 to 60 min at 1000 °C.

3.2. Surface morphology

Fig. 3a shows the back-scattered electron image of Ti_3SiC_2 coated with 40 μm Cu after annealing at 900 °C for 30 min. The gray grain-marked TSC, dark grain-marked TC, and white particles are Ti_3SiC_2 substrate, TiC_x and Cu_3Si, respectively, which were identified by analyzing the EDS spectra in Fig. 3b–d. As shown in Fig. 3a, the dark grain of TiC_x is surrounded by the white particles of Cu_3Si, which indicates that Ti_3SiC_2 reacted with Cu to form Cu_3Si leaving a cubic phase of TiC_x. Another characteristic can be observed in Fig. 3a is the appearance of grain boundary of Ti_3SiC_2, which is due to the diffusion of Cu and the formation of a new phase at the grain boundaries. In order to recognize the new phase, line scan across the grain boundaries was conducted and the result was presented in Fig. 4.

Fig. 4 shows the back-scattered electron image of a 40-μm Cu-coated Ti_3SiC_2 after annealing at 1000 °C for 60 min and the concentration profile of Ti, Cu and Si along the line in Fig. 4a. The most impressing character in Fig. 4 is that the Cu content across the grain boundaries, as marked G1, G2, G3, G4 and G5, is much higher, while the Ti and Si content at these positions are relatively low. These results imply that Cu diffused along the grain boundary into Ti_3SiC_2 substrate and reacted with Si at the grain boundary to form Cu_3Si.

3.3. Cross-section microstructure

From the above results, it is known that both the white particles and the grain boundary phase are Cu_3Si. Fig. 5a–d shows the back-scattered electron images of cross-sections of Ti_3SiC_2 coated with 40 μm Cu after annealing at the temperature range of 900–1100 °C for 30–60 min. As shown in Fig. 5a, the diffusion distance of Cu is more than 100 μm in the sample annealed at 900 °C. While in Fig. 5b, the amount of white particles pronounced increased compared with that in Fig. 5a, indicating the amount of Cu diffused further inward the Ti_3SiC_2 substrate at 1000 °C. At 1100 °C (Fig. 5c), besides white particles, the white grain boundary phase is clearly observed. Thus, we can conclude that the distance and amount of Cu diffused inward the Ti_3SiC_2 substrate increases with increasing annealing temperature. Similar trend is seen in Fig. 5d by prolonging the duration to 60 min at 1100 °C.

In order to identify the diffusion path of Cu, high-magnification images were also observed as shown in Fig. 6. At 900 °C (in Fig. 6a), white Cu_3Si particles with regular shape, e.g. triangle particles, can be observed which reveals that Cu diffused along the defects and grain boundary of Ti_3SiC_2 substrate and accumulated at the gap between adjacent Ti_3SiC_2 grains first. At higher temperature of 1100 °C, a reticular structure is formed as shown in Fig. 6b, which reveals that considerable amount of Cu diffused into Ti_3SiC_2 and filled up the grain boundaries.

3.4. Microhardness

Microhardness with the relationship of (a) thickness of Cu films, (b) heat treatment temperatures, and (c) heat treatment duration are shown in Fig. 7. It can be observed from Fig. 7a that the surface of Ti_3SiC_2 was strengthened from 5.08 GPa to a maximum of 9.65 GPa after annealing and the microhardness of the annealed samples increases with increasing the thickness of Cu films, which are consistent with the relative amount of TiC_x. While in Fig. 7b, the microhardness increases with increasing annealing temperature and a plateau appears at 1000 °C followed by a slight drop with further increasing the annealing temperature to 1100 °C. In Fig. 7c, an increase in hardness can be observed after annealing for 30 min, while a decrease is seen with further prolonging the duration to 60 min for samples annealed at 900–1100 °C. The analogous trend of microhardness versus heat treatment temperatures and duration is also consistent with that of relative amount of TiC_x. Therefore, higher microhardness can be expected when the amount of TiC_x is relatively higher. Meanwhile, owing to the discontinuity of TiC_x, the corresponding standard deviation becomes bigger after annealing.

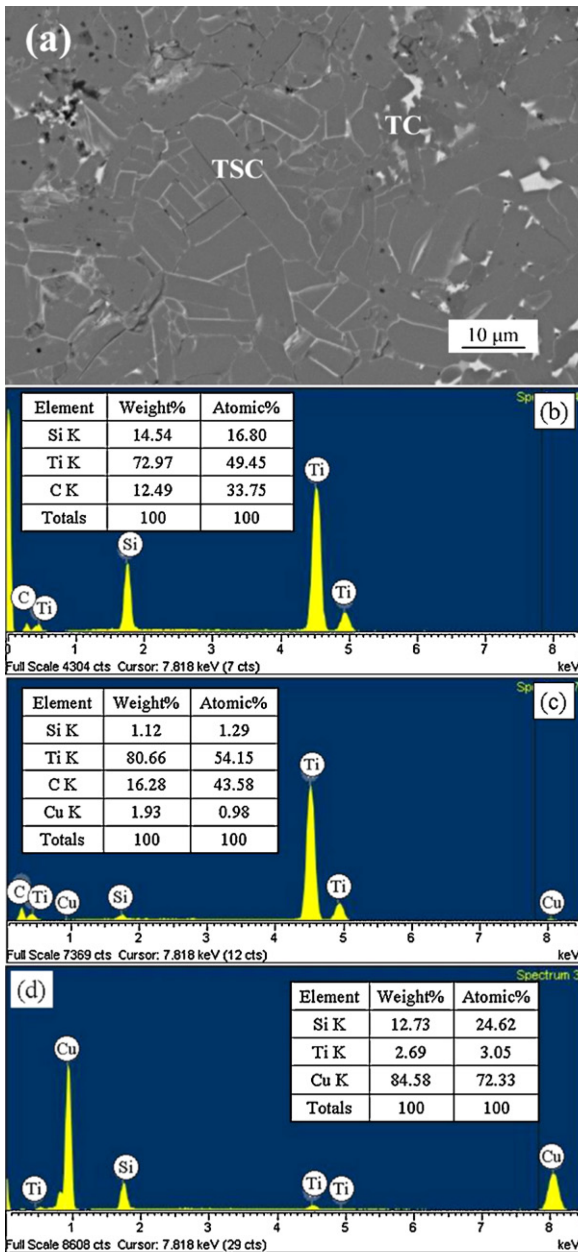

(b)

Element	Weight%	Atomic%
Si K	14.54	16.80
Ti K	72.97	49.45
C K	12.49	33.75
Totals	100	100

(c)

Element	Weight%	Atomic%
Si K	1.12	1.29
Ti K	80.66	54.15
C K	16.28	43.58
Cu K	1.93	0.98
Totals	100	100

(d)

Element	Weight%	Atomic%
Si K	12.73	24.62
Ti K	2.69	3.05
Cu K	84.58	72.33
Totals	100	100

Fig. 3. (a) Back-scattered electron image of Ti_3SiC_2 coated with 40 μm Cu after annealing at 900 °C for 30 min, (b) EDS of the gray grain marked TSC in (a), (c) EDS of the dark grain marked TC in (a), and (d) EDS of the white particles in (a).

3.5. Tribological Properties

Fig. 8 plots the frictional behavior of Ti_3SiC_2 and Ti_3SiC_2 with 40 μm Cu coating after annealing at 1000 °C for 30 min (termed as surface strengthened Ti_3SiC_2 for short) fretted against steel under the load of (a) 5 N and (b) 1 N, respectively. From Fig. 8, it can be noted that during the steady stage the COF of Ti_3SiC_2/steel and surface strengthened Ti_3SiC_2/steel are equivalent, lies around 0.4 and 0.5∼0.6 for the fretting load of 5 N and 1 N, respectively (see Table 5). The only difference between them is that the latter has lower COF (0.18 for 5 N, 0.23 for 1 N) at the running-in stage. From the surface roughness shown in Fig. 9, it is evident that the abrasive grooves of Ti_3SiC_2/steel are deeper than that of surface strengthened Ti_3SiC_2 steel both under the fretting loads of 5 N and 1 N. Consequently, in the present case the wear rates of Ti_3SiC_2/steel are higher than that of Cu-coated Ti_3SiC_2 after annealing against steel under 1 N or 5 N. The wear rates are calculated and listed in Table 5.

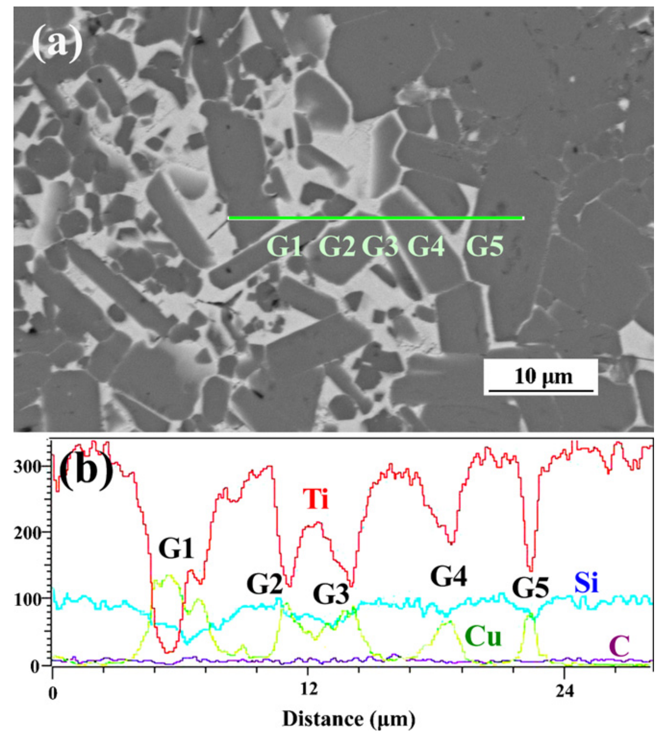

Fig. 4. (a) Back-scattered electron image of Ti_3SiC_2 coated with 40 μm Cu after annealing at 1000 °C for 60 min, (b) EDS line scans taken along the straight line shown in (a).

4. Discussions

It is known that Si is de-intercalated from Ti_3SiC_2 in the presence of Cu at high temperatures. The de-intercalation of Si from Ti_3SiC_2 causes the decreasing of c-axis and results in the volume shrinkage.[5,10] From Table 3, it can be seen that the lattice constants of Ti_3SiC_2 decreases after annealing, especially for the c-axis. Therefore, Cu-coated Ti_3SiC_2 transformed to sub-stoichiometric $Ti_3Si_xC_2$, i.e. $x < 1$, at elevated temperature by the de-intercalation of Si. When the Si content of the defective Ti_3SiC_2 is seriously reduced, i.e. less than the threshold Si content constituted of Ti_3SiC_2 layered structure, the topological transformation from hexagonal Ti_3SiC_2 to cubic TiC_x happens. Similarly, in the previous investigation of structure stability of Ti_3AlC_2 in Cu,[17] the reaction was determined to be diffusion of Al from Ti_3AlC_2 into Cu to form Cu(Al) solid solution first, while Ti_3AlC_2 retained its structure under the partial loss of Al. And then further depletion of Al resulted in highly defective Ti_3AlC_2. When all Al was removed, Ti_3AlC_2 decomposed and transformed into cubic TiC_x.

Theoretically, the transformed TiC_x ($x = 0.67$) is sub-stoichiometric. Here the 'x' value can be calculated by the

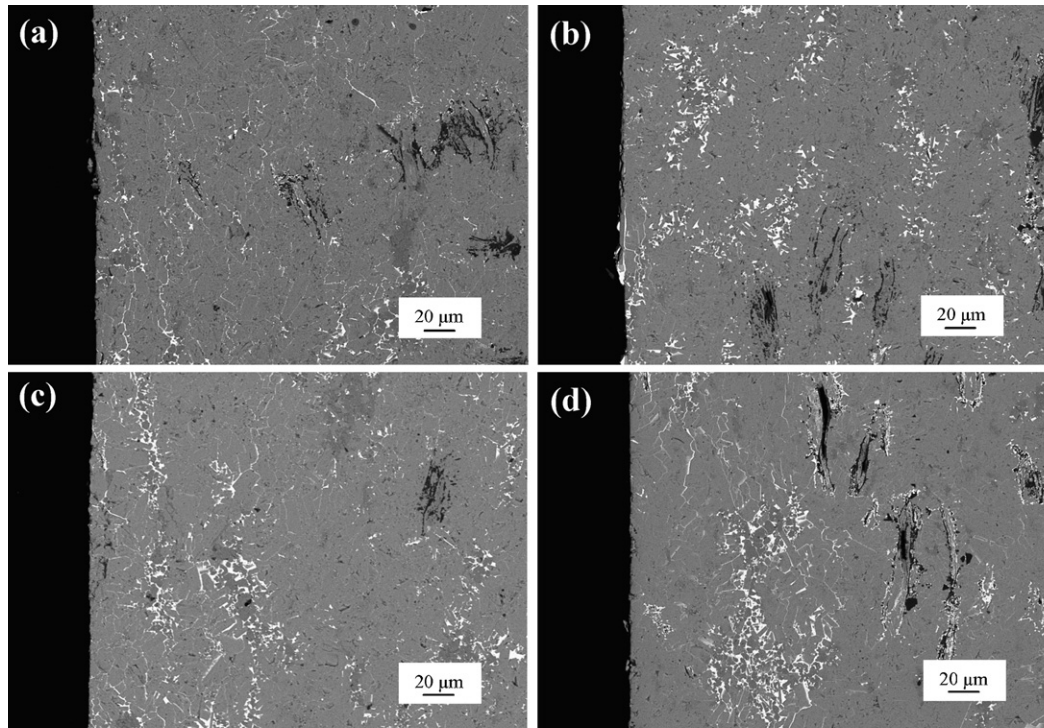

Fig. 5. Back-scattered electron images of the cross-section of Ti_3SiC_2 coated with 40 μm Cu after annealing at (a) 900 °C, (b) 1000 °C, (c) 1100 °C for 30 min and (d) 1100 °C for 60 min, showing the distribution of Cu.

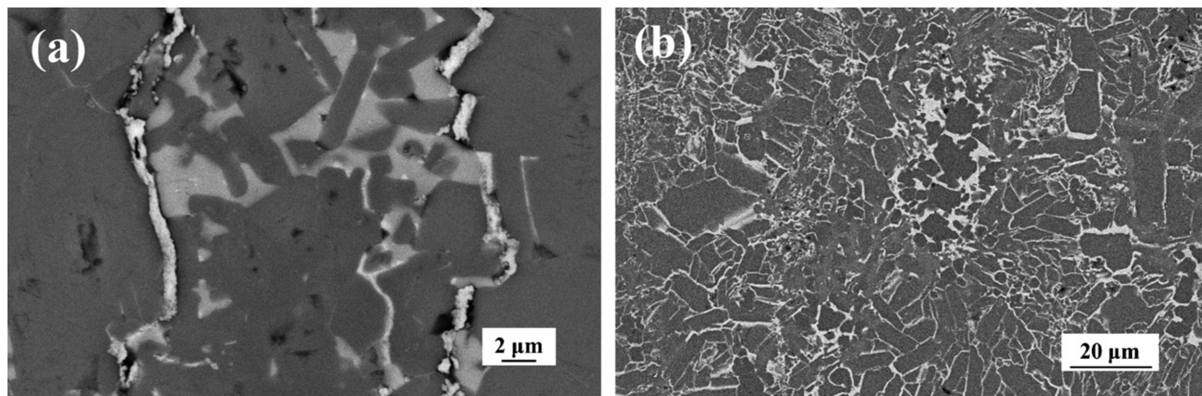

Fig. 6. High-magnification images of cross-section of Cu-coated Ti_3SiC_2 after annealing at (a) 900 °C and (b) 1100 °C for 60 min, showing the diffusion path of Cu.

reported variation of lattice spacing with composition of TiC_x by Ehrlich (1949)[18] as listed in Table 3. It can be seen that after annealing the value x is lower than that of the stoichiometric TiC. The reduced tendency implies that the occurrence of the transformation from Ti_3SiC_2 to TiC_x. But the value x for the 40 μm Cu-coated Ti_3SiC_2 after annealing at 1000 °C for 60 min is equal to 1, which implies that the transformation is mild and the as-formed TiC_x is relatively less.

In the previous work,[8] the chemical reaction between Ti_3SiC_2 and Cu at elevated-temperature could form various Cu–Si intermetallic compounds, such as Cu_5Si, Cu_5Si_4 and $\eta(Cu_3Si)$. While in the present study, a single copper silicide Cu_3Si was obtained. The formation mechanism of Cu_3Si can be explained as follows. Here a thin Cu film was used, i.e. the relative amount of Cu is less while Si is excessive. Therefore, the copper silicide with more content of Si is preferential to form. From the binary phase diagram of Cu–Si,[19] it is known that there are six kinds of copper silicide including Cu(Si) solid solution (Table 4). As shown in Table 4, Cu_3Si contains maximum amount of Si among all the copper silicides. Thus Cu_3Si is formed at the

Table 4
Atomic percentage of Si in copper silicide

	Composition, at.% Si
Cu(Si)	0–1.5
Cu_7Si	11.05–14.5
Cu_5Si	17.15–17.6
Cu_4Si	17.6–19.6
$Cu_{15}Si_4$	21.2–21.3
Cu_3Si	22.2–25.2

Table 5
Coefficient of friction and wear rate of Ti_3SiC_2 and surface-strengthened Ti_3SiC_2

Materials	Load (N)	COF			Wear rate ($mm^3/(N\,m)$)
		Running-in	Duration	Steady	
Ti_3SiC_2	1	Not visible		0.46 ± 0.03	3.26×10^{-2}
Ti_3SiC_2 after treated	1	0.23 ± 0.01	1000–2500 s	0.58 ± 0.02	2.19×10^{-3}
Ti_3SiC_2	5	Not visible		0.43 ± 0.02	7.38×10^{-3}
Ti_3SiC_2 after treated	5	0.18		0.38 ± 0.07	1.30×10^{-3}

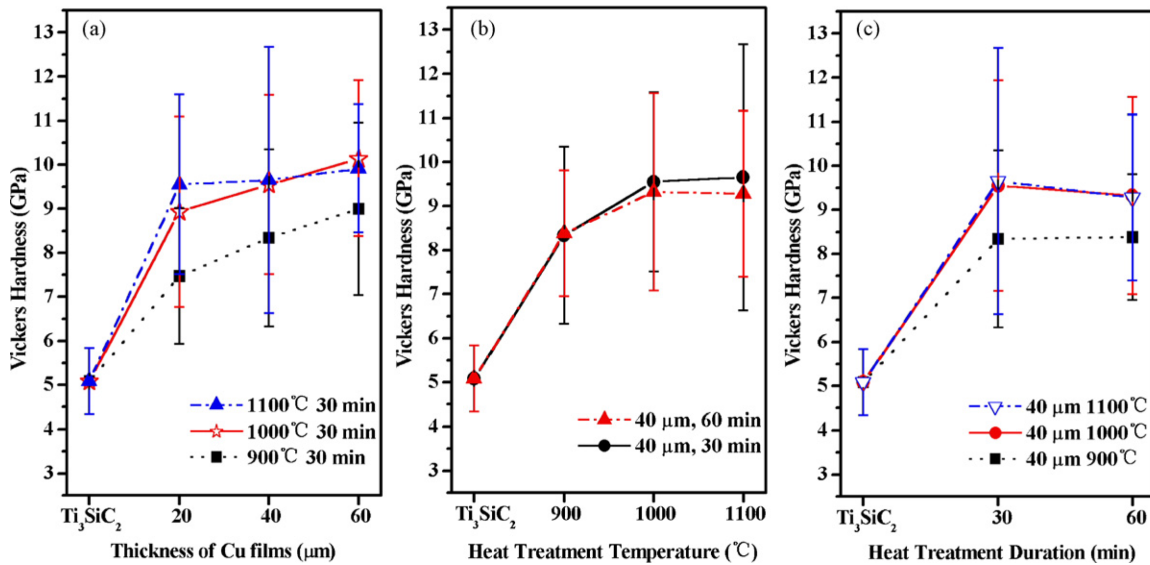

Fig. 7. (a) Microhardness vs. thickness of Cu films, (b) microhardness vs. heat treatment temperature, and (c) microhardness vs. heat treatment duration.

present condition. Whereas the microhardness of Cu_3Si was reported by Olofinjana[20] to be ∼3 GPa under a load of 15 g, which is lower in comparison with Ti_3SiC_2. Hence, there is no contribution to the surface strengthening of Ti_3SiC_2. On the other side, the molar amount of Cu_3Si is two times lower than that of as-formed TiC. So the effect of Cu_3Si is not taken into account.

From the results in the previous section, it is known that the relative amount of TiC_x is dependent on Cu film thickness, heat treatment temperature and annealing time. As shown in Fig. 10a, it increases with the increasing thickness of Cu film, which indicates that the amount of Cu is an important factor in affecting the reaction between Ti_3SiC_2 and Cu. While in Fig. 10b, it increases with the increasing annealing temperature below 1000 °C and then decreases a little bit at 1100 °C. Similarly in Fig. 10c, it increases after annealing for 30 min and then decreases with prolonging the duration to 60 min. In general, enhancing the heat treatment temperature and prolonging the duration, the

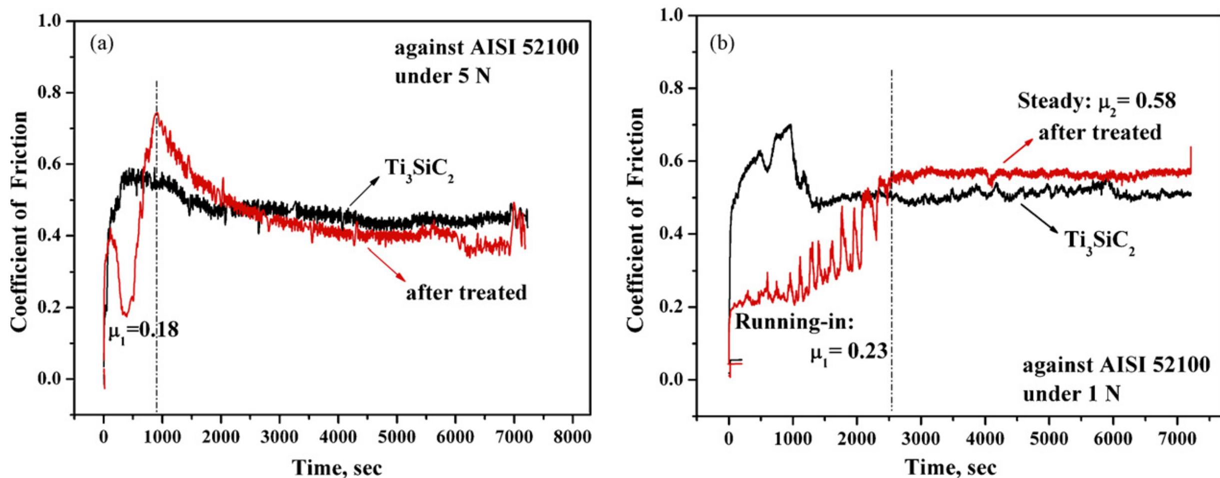

Fig. 8. Evolution of friction coefficient vs. sliding time under (a) 5 N and (b) 1 N.

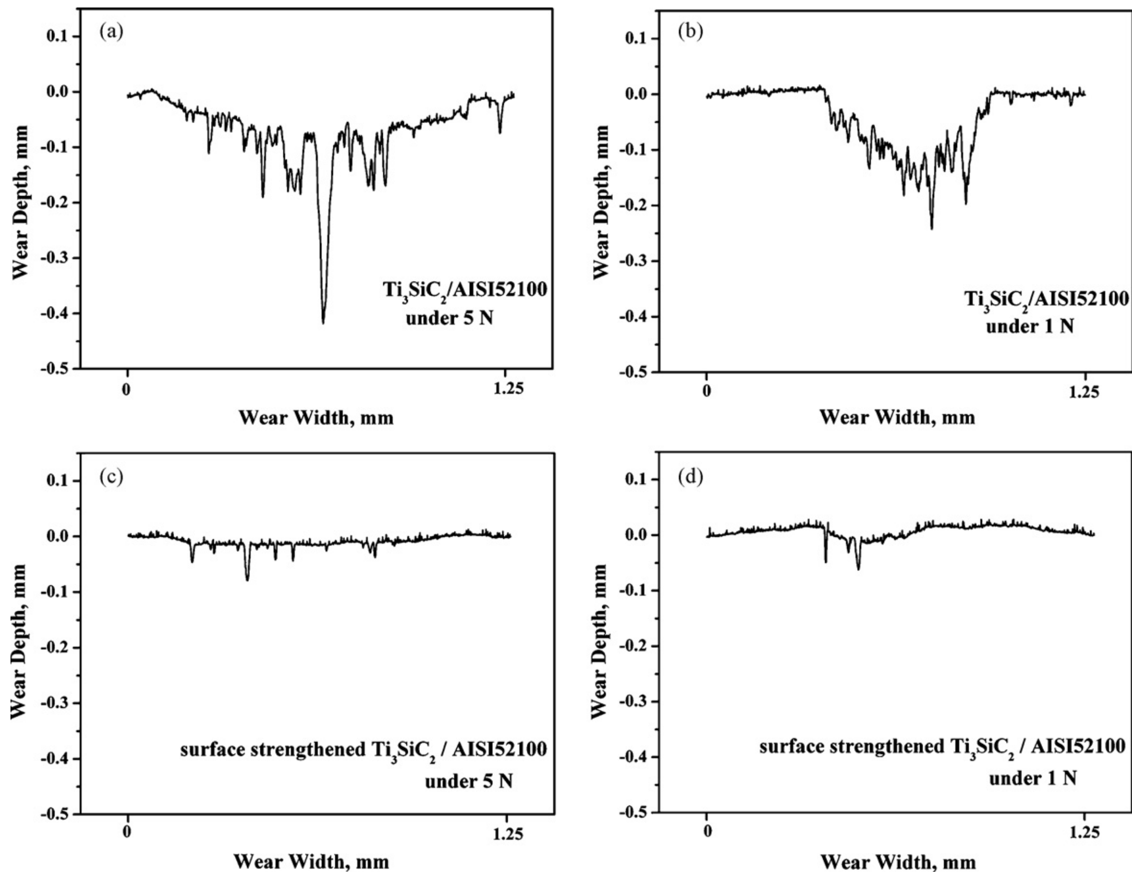

Fig. 9. Surface roughness of Ti_3SiC_2 slip wear under 5 N (a) and 1 N (b); surface roughness of the surface strengthened Ti_3SiC_2 slip wear under 5 N (c) and 1 N (d).

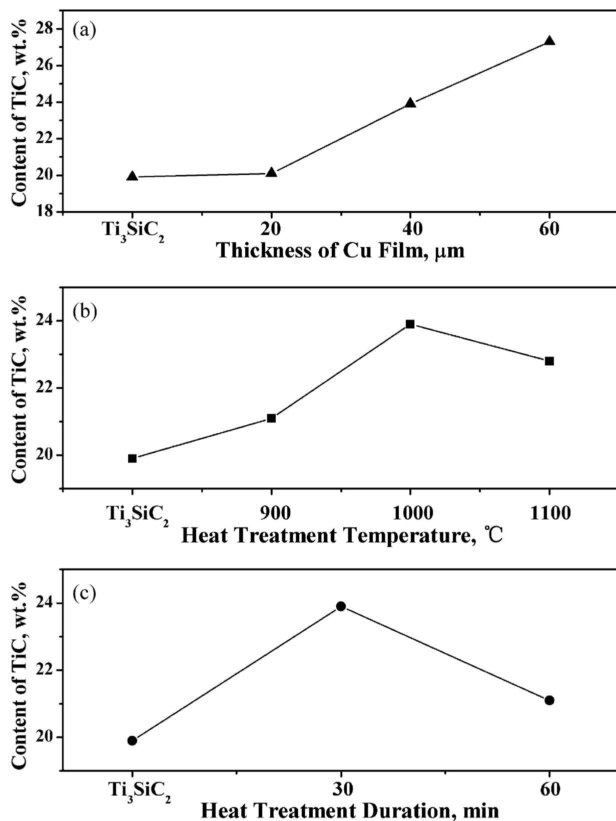

Fig. 10. Evolution of the relative amount of TiC_x vs. (a) thickness of Cu films, (b) heat treatment temperature and (c) heat treatment duration.

reaction becomes stronger. However, Cu is fairly active at high temperature and diffuses towards Ti_3SiC_2 substrate intensively. At higher temperature or longer duration, more amount of Cu diffused inward the Ti_3SiC_2 substrate. In addition, Cu may be volatilized at 1100 °C above its melting point (1083 °C). So that the relative amount of Cu near the surface reduced. Therefore, the interfacial reaction products between Cu layer and Ti_3SiC_2 substrate at surface becomes less at 1100 °C or with prolonging the duration to 60 min. Owing to the dependence of the relative amount of TiC_x on microhardness, the maximal microhardness is expected to obtain at 1000 °C for 30 min. It is really disappointing that the corresponding standard deviation is large which is strongly dependent on the distribution of TiC_x. It can be seen from Fig. 3a that TiC_x is accompanied by Cu. In other words, the presence of Cu at the grain boundary induced de-intercalation of Si from Ti_3SiC_2 to form TiC_x and the diffusion ability of Cu is so strong that the formed TiC_x is discontinues.

The tribological results revealed that surface strengthened Ti_3SiC_2/steel presents equivalent COF at the steady stage but lower COF at the running-in stage compared with Ti_3SiC_2/steel couple, regardless of the load. Moreover, surface strengthened Ti_3SiC_2 has lower wear rate. In the previous investigation of fretting wear of Ti_3SiC_2,[21] the major mechanisms contributing to the process of friction and wear includes: (a) abrasion, (b) tribochemical layer formation and (c) plastic deformation. Compared with monophase Ti_3SiC_2, the improvements of both the running-in stage COF and the wear rate of surface strengthened Ti_3SiC_2 are attributed to the formation of TiC_x.

5. Conclusions

In order to improve the surface hardness and wear resistance of Ti_3SiC_2, magnetron-sputtering deposition Cu and subsequent annealing were conducted in the temperature range of 900–1100 °C for 30–60 min. Owing to the formation of TiC_x following the reaction $Ti_3SiC_2 + 3Cu \rightarrow 3TiC_{0.67} + Cu_3Si$, the surface hardness was enhanced from 5.08 GPa to a maximum 9.65 GPa. The relative amount of TiC depends on three factors, thickness of Cu films, heat treatment temperatures and annealing times. First, it increases with the increasing thickness of Cu film. Second, it increases with increasing heat treatment temperature below 1000 °C while decreases at 1100 °C. Third, it increases with increasing the duration below 30 min while decreases with prolonging the duration to 60 min. Furthermore, Ti_3SiC_2 with 40 μm Cu-coating after annealing at 1000 °C for 30 min has lower wear rate and lower COF at the running-in stage compared with Ti_3SiC_2 substrate. The reaction between Ti_3SiC_2 and Cu is triggered by the pronounced interdiffusion of Cu and Si. Cu diffuses inward Ti_3SiC_2 along the grain boundaries and accumulates at the trigonal holes of Ti_3SiC_2 first. When considerable amount of Cu diffused to Ti_3SiC_2, it fills up the grain boundaries leaving a mesh structure. While in the presence of Cu, Si tends to de-intercalate from Ti_3SiC_2 along the basal plane. Cu-coated Ti_3SiC_2 is transformed to substoichiometric $Ti_3Si_xC_2$, i.e. $x < 1$, first. When the Si content of the defective Ti_3SiC_2 is seriously reduced, i.e. less than the threshold Si content constituted of Ti_3SiC_2 layered structure, the topological transformation from hexagonal Ti_3SiC_2 to cubic TiC_x happens.

Acknowledgements

This work was supported by the National Outstanding Young Scientist Foundation for Y.C. Zhou under Grant no. 59925208, Natural Sciences Foundation of China under Grant no. 50232040, no. 50302011, no. 90403027, and ‘863’ project.

References

1. Barsoum, M. W. and El-Raghy, T., Synthesis and characterization of a remarkable ceramic: Ti_3SiC_2. *J. Am. Ceram. Soc.*, 1996, **79**, 1953–1956.
2. El-Raghy, T., Zavaliangos, A., Barsoum, M. W. and Kalidindi, S. R., Damage mechanisms around hardness indentations in Ti_3SiC_2. *J. Am. Ceram. Soc.*, 1997, **80**, 513–516.
3. Zhou, Y. C., Sun, Z. M., Chen, S. Q. and Zhang, Y., In situ hot pressing/solid-liquid reaction synthesis of dense titanium silicon carbide bulk ceramics. *Mater. Res. Innovat.*, 1998, **2**, 142–146.
4. Barsoum, M. W., The $M_{N+1}AX_N$ phases: a new class of solids; thermodynamically stable nanolaminates. *Prog. Solid State Chem.*, 2000, **28**, 201–281.
5. El-Raghy, T. and Barsoum, M. W., Diffusion kinetics of the carburization and silicidation of Ti_3SiC_2. *J. Appl. Phys.*, 1998, **83**, 112–119.
6. Li, C., Li, M. S. and Zhou, Y. C., Improving the surface hardness and wear resistance of Ti_3SiC_2 by boronizing treatment. *Surf. Coat. Technol.*, 2006, **201**, 6005–6011.
7. Zhou, Y. C. and Sun, Z. M., Crystallographic relations between Ti_3SiC_2 and TiC. *Mater. Res. Innovat.*, 2000, **3**, 286–291.
8. Zhou, Y. C. and Gu, W. L., Chemical reaction and stability of Ti_3SiC_2 in Cu during high-temperature processing of Cu/Ti_3SiC_2 composites. *Z. Metallkd.*, 2004, **95**, 50–56.
9. Yin, X. H., Li, M. S. and Zhou, Y. C., Microstructure and mechanical strength of diffusion bonded Ti_3SiC_2/Ni joints. *J. Mater. Res.*, 2006, **9**, 2415–2421.
10. Barsoum, M. W., El-Raghy, T., Farber, L., Amer, M., Christini, R. and Adams, A., The topotactic transformation of Ti_3SiC_2 into a partially ordered cubic $Ti(C_{0.67}Si_{0.06})$ phase by the diffusion of Si into molten cryolite. *J. Electrochem. Soc.*, 1999, **146**, 3919–3923.
11. El-Raghy, T., Barsoum, M. W. and Sika, M., Reaction of Al with Ti_3SiC_2 in the 800–1000 °C temperature range. *Mater. Sci. Eng. A*, 2001, **298**, 174–178.
12. Chan, K. Y., Tou, T. Y. and Teo, B. S., Thickness dependence of the structural and electrical properties of copper films deposited by dc magnetron sputtering technique. *Microelectron. J.*, 2006, **37**, 608–612.
13. Young, R. A., *The Rietveld Method*. Oxford University Press, Oxford, UK, 1993, p. 1.
14. Musil, J., Kunc, F., Zeman, H. and Polakova, H., Relationships between hardness. Young's modulus and elastic recovery in hard nanocomposite coatings. *Surf. Coat. Technol.*, 2002, **154**, 304–313.
15. Yang, C. Y., Jeng, J. S. and Chen, J. S., Grain growth, agglomeration and interfacial reaction of copper interconnects. *Thin Solid Films*, 2002, **420–421**, 398–402.
16. Kuo, Y. L., Lee, C., Lin, J. C., Yen, Y. W. and Lee, W. H., Evaluation of the thermal stability of reactively sputtered (Ti, Zr)N_x nano-thin films as diffusion barriers between Cu and silicon. *Thin Solid Films*, 2005, **484**, 265–271.
17. Zhang, J., Wang, J. Y. and Zhou, Y. C., Structure stability of Ti_3AlC_2 into Cu and microstructure evolution of Cu–Ti_3AlC_2 composites. *Acta Mater.*, 2007, **55**, 4381–4390.
18. Pearson, W. B., *A Handbook of Lattice Spacing and Structures of Metals and Alloys*. Pergamon Press, London, 1958, p. 949.
19. Olesinski, R. W. and Abbaschian, G. J., (*2nd ed.*). *Binary Alloy Phase Diagrams*, *vol. 2*ASM International, 1990, p. 1477.
20. Olofinjana, A. O. and Atrens, A., Properties of rapidly solidified binary copper alloys. *Mater. Lett.*, 1997, **31**, 87–92.
21. Sarkar, D., Mgnoj Kumar, B. V. and Basu, B., Understanding the fretting wear of Ti_3SiC_2. *J. Eur. Ceram. Soc.*, 2006, **26**, 2441–2452.